European Journal of Molecular & Clinical Medicine
ISSN 2515-8260 Volume 07, Issue 08, 2020

Methemetical Modeeling And Validation Of Thermosymphon With Permofrost Used On Solar Radiation With Moisture

Ravish Kumar Srivastava[1], Anil Kumar[2] and Bikas Prasad[3]

[1]Professor,
Mechanical Engg.
Deptt. SITE, Swami Vivekanand Subharti University, Meerut, (U.P.), India
Email: rk_281@rediffmail.com

[2]Professor,
Mathematics Deptt.
SITE, Swami Vivekanand Subharti University, Meerut, (U.P.), India
dranilkumar73@rediffmail.com

[3.] Principal,
Govt. Polytechnic Dehri-on-sone, Rohtas,Bihar

[1]corresponding author
2010 Mathematics Subject Classification. 03C65,60H35.

ABSTRACT:
The scope of the investigation is to validate the combined functioning of double phase thermosyphon –soil-atmosphere in arctic area. In this area permafrost phases the considerable amount of problem on account of geometrical consideration with moisture. Defrosting process helps to reduce volume and irregular foundation. In order to overcome this two phase vertical type thermosyphons are introduced. It transfer low temperature with moisture from atmosphere to the ground surface without consumption of power. Here an attempt is made to develop a mathematical model for average film thickness of refrigerant available on all inner portion of the thermosyphon such as over and underground heat insulated pipe , evaporator etc. Mathematical analysis and study predicts that the resistance of refrigerants have been two times lesser then the condenser. Thus the experimental calculations of soil temperature at different regime made possible without consideration of refrigerant film thickness. The relation for solar radiation components for condenser and over ground pipe is developed. A comparative analysis of two models of system double phase thermosyphon – soil – atmosphere predicts that the introduced model lowers the freezing radius the maximal distance in between thermosyphons is about 18.6 %.

Key words and phrases. Permafrost, heat transfer mechanism in soil, thermosyphon, solar radiation, freezing radius.

INTRODUCTION

An attempt is made to analyze the performance of combined operation of system: 2-phase thermosyphon – soil – atmosphere. 2- phase thermosyphons are used to lowered the temperature of permafrost in areas with arctic climate & to stabilize the subsidence of foundations at different structures: buildings & pipelines [1-5]. The design is used to reduce energy consumption in the winter time in areas with hot climate [6].

The researchers and scientists have been contributed towards the area of vertical thermosyphons, which are discussed in review articles of Jafari, and Jadhav. [7-8]. Haan investigated the methods of thermodynamic computation of vertical thermosyphons [9-10]. Özba investigated the influence of study of fluid to the performance of thermosyphon [11]. Gorelik investigated the influence offering to the heat transmission and performance of thermosyphon [12]. AliK.et al. studied the influence of channel shape to heat transmission [13-15]. On the basis of extensive study there is a gap in the study of their efficiency in permafrost. There is no estimates of the influence of liquid refrigerant film on the soil freezing radius taking into the account real climatic conditions. In the same way, there is no valid formulas & studies that allow to estimate the effect of solar radiation i.e. (Direct, diffuse, & reflected) on the freezing radius. This is probably due to the fact that the value of solar radiation in the Arctic is low. The micro level work to calculate the freezing radius is the work of Gorelik Ya.B. [12]. Therefore, everywhere , the comparison of the introduced model and the model in [12] was developed.

In present study the mathematical model is developed to investigate the model:

1) Mathematical model developed to analyze the thermal regime of the soil around of a vertical two-phase thermosyphon with moisture.

2) Method for calculating the absorbed solar radiation by the condenser & overground pipe taking into account the available irradiance data;

3) Investigating the analytical deviation of soil freezing near thermosymphon excluding thermal resistance of liquid film of refrigerant near the inner place of the surface.

4) Estimating the difference in the calculation of soil freezing radius around different type of radiation [12].

2. MATERIAL AND METHODS

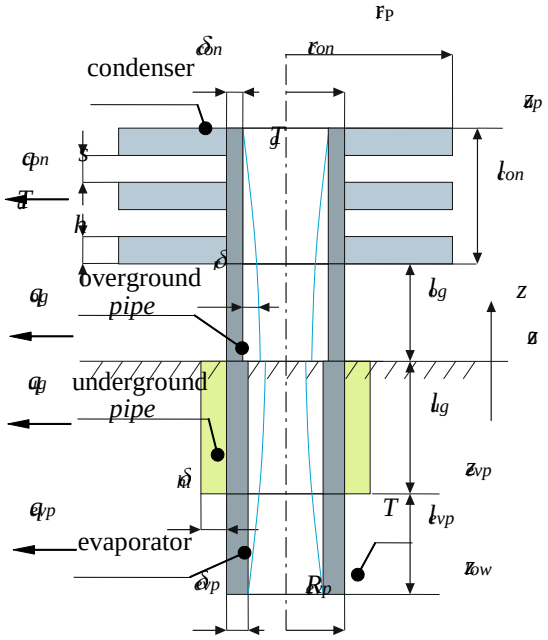

Figure 1. Figure of modified two-phase thermosyphon

The mathematical model is represented here on the basis of given assumption:

1) The nature of heat transfer in the thermosyphon is quasi-stationary.

2) Nusselt number is the deciding factor of quantity of liquid film.

3) Refrigerant vapor is insignificant on account of supercooling, interns it is possible to equate the heat flux to the rate of evaporation-condensation taking into account the heat of phase transition.

In the mathematical modeling the basic heat balance equation for thermosymphon is used :

$$\int_{z_{low}}^{z_{up}} Q_t dz - e_{sun} - m = 0 \qquad (1)$$

On the basis of construction shown in fig 1 , the thrmosymphon is divided in to four parts :

1) At the condition of refrigerant vapor condensation , heat transfer to the atmosphere through condenser

2) A considerable small amount of heat transfer to the atmosphere from the ground pipe surface it helps to rise condenses over the snow cover.

3) The transfer of liquid refrigerant to the bottom without heat losses is possible by underground pipes.

4) When refrigerant evaporates, Evaporator extract heat from the soil.

Then equation (1) can be termed as the sum of heat balance :

$$\left(Q_{con}L_{con} + Q_{og}L_{og}\right) + \int_{z_{evp}}^{z_0} Q_{ug} dz + \int_{z_{down}}^{z_{evp}} Q_{ug} dz - e_{sun} - m = 0 \qquad (2)$$

Through Newton's law of cooling equation 2 can be written as based on the parameter like change in temperature in between primary temperature and gaseous phase of refrigerant :

$$\left(k_{con}L_{con} + k_{og}L_{og}\right)\left(t_g - t_{air}\right) + k_{ug}\left(t_g L_{ug} - \int_{z_{evp}}^{z_0} t dz\right) +$$

$$k_{evp}\left(L_{evp}t_g - \int_{z_{down}}^{z_{evp}} t dz\right) - e_{sun} - m = 0 \qquad (3)$$

From equation (3) one can obtain the temperature of gaseous phase of refrigerant:

$$t_g = \frac{\left(k_{con}L_{con} + k_{og}L_{og}\right)t_{air} + k_{ug}\int_{z_{evp}}^{z_0} t dz + k_{evp}\int_{z_{low}}^{z_{evp}} t dz + e_{sun}}{k_{con}L_{con} + k_{og}L_{og} + k_{ug}L_{ug} + k_{evp}L_{evp}} \qquad (4)$$

By using equation (4), calculate the heat flux in the zone of interaction between the thermosyphon & soil:

$$Q_{evp} = k_{evp}\left(t_g - t_{soil}\right) \qquad (5)$$

$$Q_{ug} = k_{ug}\left(t_g - t_{soil}\right) \qquad (6)$$

The basic equations for heat transfer coefficients k_{con}, k_{og}, k_{ug}, k_{evp} at all segment of thermosyphon:

$$k_{con} = \left(\frac{L_{con}}{N\left(\tau_n s_n + 2\pi r_{con} H \lambda r \vartheta \omega\right)} + \frac{1}{2\pi\eta_{con}} ln\left(\frac{r_{con}}{r_{con} - \psi_{con}}\right) + + \frac{1}{2\pi\eta_{rf}} ln\left(\frac{r_{con} - \psi_{con}}{r_{con} - \psi_{con} - \psi_{rca}}\right)\right)^{-1}$$

(7)

$$k_{og} = \left(\frac{1}{2\pi\eta_{con}} ln\left(\frac{r_{con}}{r_{con} - \psi_{con}} \right) + \frac{1}{2\pi\eta_{rf}} ln\left(\frac{r_{con} - \psi_{con}}{r_{con} - \psi_{con} - \psi_{roa}} \right) \right)^{-1} \quad (8)$$

$$k_{ug} = \left(\frac{1}{2\pi\eta_{H_i}} ln\left(\frac{r_{evp} + \psi_{hi}}{r_{evp}} \right) + \frac{1}{2\pi\eta_{evp}} ln\left(\frac{r_{evp}}{r_{evp} - \psi_{evp}} \right) + \right.$$

$$\left. + \frac{1}{2\pi\eta_{Rf}} ln\left(\frac{r_{evp} - \psi_{evp}}{r_{evp} - \psi_{evp} - \psi_{rua}} \right) \right)^{-1} \quad (9)$$

$$k_{evp} = \left(\frac{1}{2\pi\eta_{evp}} ln\left(\frac{r_{evp}}{r_{evp} - \psi_{evp}} \right) + \frac{1}{2\pi\eta_{rf}} ln\left(\frac{r_{evp} - \psi_{evp}}{r_{evp} - \psi_{evp} - \psi_{rea}} \right) \right)^{-1} \quad (10)$$

$$\omega = \frac{k_1(\phi r_{con}) a_\phi - i_1(\vartheta r_{con}) b_\omega}{K_0(\mu R_{con}) a_\psi + I_0(\phi r_{con}) b_\omega} - m \quad (11)$$

$$A_\omega = \eta_r \phi i_1(\phi r_R) + \tau_R i_0(\phi r_R) \quad 12)$$

$$B_\omega = \eta_r \omega k_1(\vartheta r_R) - \tau_R k_0(\vartheta r_R) \quad (13)$$

$$\phi = \sqrt{2\tau_r / \eta_R H} \quad (14)$$

$$s_N = 2\pi r_{con} S \quad (15)$$

$$\tau_r = 0.036 \frac{\eta_a}{2r_R} \left(\frac{2r_R v_a}{v_a} \right)^{0,8} (\mathrm{pr}_a)^{0.42} \quad (16)$$

$$\tau_r = 0.022 \frac{\eta_a}{2r_R} \left(\frac{2r_R v_a}{v_a} \right)^{0,8} (\mathrm{Pr}_a)^{0.4} \quad (17)$$

$$\tau_n = 0.025 \frac{\eta_a}{2r_{con}} \left(\frac{2r_{con} v_a}{v_a} \right)^{0.8} (\mathrm{pr}_a)^{0.38} \quad (18)$$

Equations (11) - (14) are generated based on heat equation in thin ring plate, under boundary conditions, first type on the inner radius of the ring & third one on the other surfaces.

In equations (7) - (10), the average thickness of the film of the refrigerant in different parts of thethermosyphonδ_{rca}, δ_{roa}, δ_{rua}, δ_{rea}

The Nusselt no for film thickness:

$$\frac{\partial j}{\partial z} = -\frac{q_t}{L_{rf}} \quad (19)$$

The flow of liquid refrigerant can be found as a result of solving the approaching of Navier-Stokes equation for the free movement of fluid by gravity on a vertical surface:

$$J = \rho_{RF} 2\pi (r - \psi) \frac{g\psi_r^3}{3v_{RF}} \quad (20)$$

The expression for the film thickness:

$$\psi_r = \left\{ \psi_{r0}^3 + \frac{-3Qv_{RF}\left(Z - Z_0\right)}{\rho_{RF} g 2\pi \left(r - \psi\right) l_{RF}} \right\}^{\frac{1}{3}} \tag{21}$$

The average film thickness can be found from equation (21):

$$\psi_{RA} = \frac{\rho_{RF} g 2\pi \left(r - \psi\right) l_{RF}}{-3Qv_{RF}\left(Z - Z_0\right)} \left(\frac{3}{4} \left\{ \psi_{r0}^3 + \frac{-3Qv_{RF}\left(Z - Z_0\right)}{\rho_{RF} g 2\pi \left(r - \psi\right) l_{RF}} \right\}^{\frac{4}{3}} - \frac{3}{4} \psi_{r0}^4 \right) \tag{22}$$

Then we derived the average film thickness for each section:

$$\psi_{rca} = \frac{3}{4} \left\{ \frac{3k_{og}\left(t_g - t_{air}\right) v_{rf} l_{con}}{\rho_{RF} g 2\pi \left(r_{con} - \psi_{con}\right) l_{rf}} \right\}^{\frac{1}{3}} = \frac{3}{4} \psi_{rc} \tag{23}$$

$$\psi_{roa} = \frac{\rho_{RF} g 2\pi \left(r_{con} - \psi_{con}\right) L_{rf}}{3Qv_{RF} L_{og}} \cdot \cdot \left(\frac{3}{4} \left\{ \psi_{rc}^3 + \frac{3k_{og}\left(t_g - t_{air}\right) v_{rf} l_{og}}{\rho_{rf} g 2\pi \left(r_{con} - \psi_{con}\right) l_{RF}} \right\}^{\frac{4}{3}} - \frac{3}{4} \psi_{rc}^4 \right) \tag{24}$$

$$\psi_{rua} \approx \psi_{roa}, \tag{25}$$

$$\psi_{rea} = \frac{3}{4} \psi_{rua}. \tag{26}$$

Equation (25) considers that the section is insulated & very small heat flow. Equation (26) y obtained from (22) here the direction of integration is changed: at the stationary region the film thickness at bottom is 0.

Thus, all the unknown value from equations (7) - (10) can be obtained . It is noted that the calculation sequence is : equations (7) - (18), & (4), then (23) - (26). At this stage , the iteration cycle is repeated, until the values (23) - (26) stop changing. Statement No 1 solved.

Another method to analyze the absorbed solar radiation E_{sun} is discussed here. At the initial stage source data is required. Under the normal cloud condition, direct solar radiation on horizontal plane normal to the surface & diffuse only on horizontal surface. [16]

Direct solar radiation flux on the vertical surface :

$$s_v = \sqrt{s_{sun}^{'2} - s_{sun}^2} \tag{27}$$

One can analyse direct vertical irradiance as :

$$e_s = \gamma_{con} 2 r_R L_{con} \sqrt{s_{sun}^{'2} - s_{sun}^2} \tag{28}$$

The analysis of the flux of diffuse & reflected solar radiation is very difficult. Consider the schematic on Fig. 2: A condenser with radius R_r is irradiated by diffuse solar radiation from the height H_a. At this stage it is not assume the value of H_a.

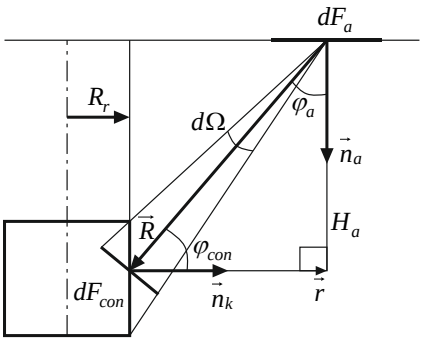

Figure 2. The fig for calculation of absorbed sun radiation by condenser & overground pipe

The area of the infinitesimal element of the cylindrical surface of the condenser:

$$df_{con} = r_R d\theta dl_{con} \tag{29}$$

In accordance with Lambert's law, one can obtained the density of the energy flow on a condenser:

$$de_d^2 = \varepsilon_{con} \frac{G_{sun}}{\pi} df_a \cos(\varphi_a) d\Omega \tag{30}$$

The solid angle :

$$d\Omega = \frac{\cos(\varphi_{con})}{|r|^2} df_{con} \tag{31}$$

After integrating (30) & taking in account (29) upon the surface of the sky in the direction where solar radiation fall on the dF_{con} surface:

$$de_d = \varepsilon_{con} \frac{G_{sun}}{\pi} \left\{ \int_0^\infty \int_0^\pi \frac{\cos(\varphi_a)\cos(\varphi_{con})}{|r|^2} d\omega r dr \right\} df_{con} \tag{32}$$

After integration:

$$de_d = \frac{\pi}{4} \varepsilon_{con} G_{sun} df_{con} \tag{33}$$

Absorbed energy of diffuse solar radiation from relation (33) & (29):

$$e_d = \frac{\pi}{4} \varepsilon_{con} G_{sun} \left(2\pi r_R L_{con}\right) \tag{34}$$

The flux of reflected solar radiation:

$$e_{ref} = \frac{\pi}{4} \varepsilon_{con} a_{surf} q_{sun} \left(2\pi r_R L_{con}\right) \tag{35}$$

$$q_{sun} = G_{sun} + s_{sun} \tag{36}$$

Energy absorbed by condenser butt is:

$$e_r = \varepsilon_{con} q_{sun} \pi r_R^2 \tag{37}$$

On Summation of (28), (34), (35) & (37) for condenser & the over ground pipe, It provides the for absorbed solar radiation by thermosyphon:

$$e_{sun} = \varepsilon_{con} q_{sun} \pi r_R^2 + 2\sqrt{s_{sun}^{'2} - s_{sun}^2} \left(\gamma_{con} r_R L_{con} + \gamma_{og} r_{con} L_{og}\right) +$$

$$+\pi\frac{\pi}{2}\left(G_{sun}+a_{surf}\,q_{sun}\right)\left(r_R L_{con}\gamma_{con}+r_{con}L_{og}\gamma_{og}\right) \qquad (38)$$

Equation (38) consider the absorption as direct, diffuse & reflected solar radiation over ground part of thermosyphon. ProblemNo 2 solved.

Another, a mathematical analysis for the soil freezing radius around thermosyphon, Is performed by using the classical example (Fig. 3). By reducing the temperature (t_{BF}– 0.5)ºC increases the strength & deformation properties of soil & is necessary for foundation in zone of discontinuous distribution of permafrost soils.

The aim of the analysis is determine the freezing radius r_{fr} The calculations is performed by using the introduced model & method, [12].

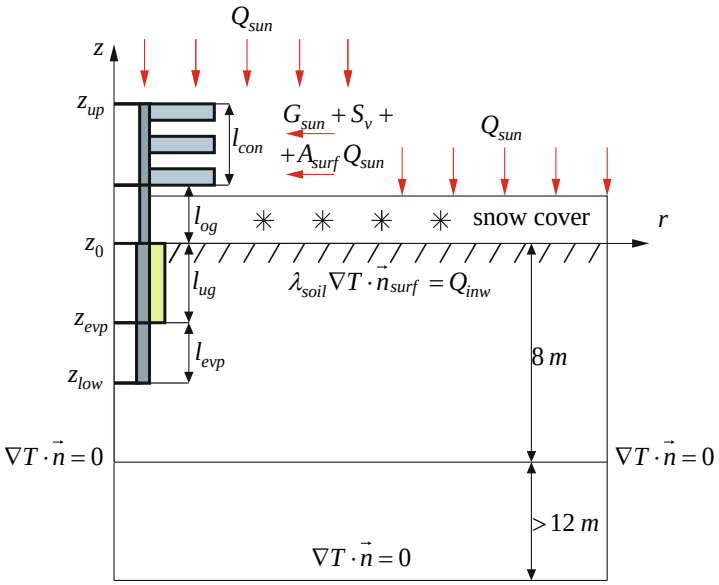

Figure 3. The calculation scheme for determining the radius of freezing around thermosyphon

The statement is analyzed by axis symmetric methodology. Thermosyphon is on the axis r = 0. The parameters of the thermosyphon are given in Table 1. The thermosyphon in total length of 8m,built up of MS, & filled up by ammonia. Soil properties are given in Tables 2-3. Atmospheric conditions as in Delhi & are shown in Table 4. The solar radiation parameters are given in Table 5.

Nonlinear heat equation is used for the mathematical investigation [17]:

$$\left(\rho_{soil}C_{soil}+l_W\frac{\partial\rho_w}{\partial T}\right)\frac{\partial T}{\partial t}=\nabla\cdot\left(\eta_{soil}\nabla T\right) \qquad (39)$$

$$\vec{Q}_{inW}\cdot\left(-\vec{n}_{surf}\right)=A_{surf}\left(t_{air}-t\right)+\left(1-a_{surf}\right)q_{sun}+\gamma_{surf}\sigma_0\left(b_{air}{t_{air}}^4-t^4\right) \qquad (40)$$

The methodology for analyzing thermal conductivity & isobaric heat capacity using equations [18-20].

Table 1. Thermosyphon construction parameters.

L_{con}	L_{og}	L_{ug}	l_{evp}	r_R
1.0	1.0	4.0	3.0	0.2
r_{con}	δ_{con}	r_{evp}	δ_{evp}	H
0.01685	0.0035	0.01685	0.0035	0.002

s	γ_{con}	γ_{og}	η_{con}	η_R
0.01	0.9	0.9	40	40
η_{evp}	η_{hi}	δ_{hi}	η_{rf}	ρ_{rf}
40	0.06	0.025	0.506	639
v_{rf}	L_{rf}			
2.73e-7	1.262e+6			

Table 2. Thermal properties of soils.

Soil	**Type**	c_{th}	c_{fr}	η_{th}	η_{fr}	η_{bf}	t_{int}
1	Sand	1260	950	2.57	2.83	-0.3	0.3
2	Clay loam	1487	1125	1.55	1.88	-0.1	0,8

Table 3. Physical properties of soils.

Soil	**Type**	ρ_{soil}	ρ_{sk}	$\rho_{w,tot}$	$\rho_{w,max}$	$\rho_{w,nf}$
1	Sand	2125	1800	325	325	0
2	Clay loam	2157	1800	357	357	120

Table 4. Climate & show cover.

Month	t_{air}	v_{air}	Ψ_{sn}	ρ_{sn}
1	22	5.2	39.6	220
2	17.6	7.9	38.0	235
3	18.6	5.2	43.0	244

4	12.7	4.9	35.0	272
5	3.7	3.0	7.2	342
6	4.9	7.7	0.0	0
7	11.0	3.7	0.7	137
8	9.9	5.5	0.44	203
9	4.5	5.5	1.1	0
10	3.8	7.7	3.4	145
11	12,5	7.8	21.3	178
12	17.7	4.4	27.5	229

Table 5. Solar radiation parameters.

Month	s'_{sun}, J/m^2	s_{sun}, J/m^2	G_{sun}, J/m^2	q_{sun}, J/m^2	a_{surf}, u.f.
1	23	5	15	13	0.77
2	123	22	54	68	0.72
3	339	112	132	251	0.75
4	451	211	242	441	0.67
5	482	233	353	611	0.42
6	473	253	291	552	0.23
7	554	320	223	559	0.22
8	322	151	211	355	0.23
9	17	71	12	18	0.2

	5		7	8	7
10	102	23	7	95	0.61
11	44	7	19	25	0.73
12	7	3	3	5	0.79

The temperature of soil at zero depth yearly amplitudes is 0.68 °C. To get the required temperature, Thickness coefficient of snow cover is 1.079, ie. Little increases the snow cover thickness (Table 4). The span of the analysis is 5 years. The statements were solved through FDA Methodology.

3. RESULTS AND DISCUSSION

In this investigation to solve the governing equations by using Newton mathematical technique and various combination of parameters of heat transfer obtain from sugar radiation are analyzed. The moisture contains surrounding the equipment results negligible amount of impact over the performance. Fig. 4 show that predicts the nature of time dependence of the average refrigerant film thickness in condenser.

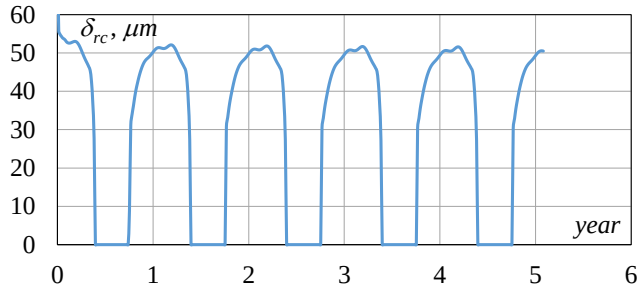

Figure 4. The time dependence of the average refrigerant film thickness in condenser

Investigation of dependence in above Figure predicts that maximum thermal resistance to the condensate film is not higher than 1.039e-4 m^2·K/W. This amount is significantly lower than the thermal resistance of the condenser, that is about 2.383e-2 m^2·K/W. The error was developed by the absence of a film in the analysis is within the error of mathematical investigation method .

Thermal resistance of refrigerant film does not affect the freezing radious. The condition of the isotherm of 0.69 ºC in the calculation without the film is not shown here, so that no visible differences during comparison to the calculation where the film was taken into account. ProblemNo 3 solved.

Fig. 5 predicts the estimated temperature distribution, in the soil around the thermosyphon.Freezing radius r_{fr} at a depth of z=-4.9m is shown. A cold temperature zone is formed near the thermosyphon.

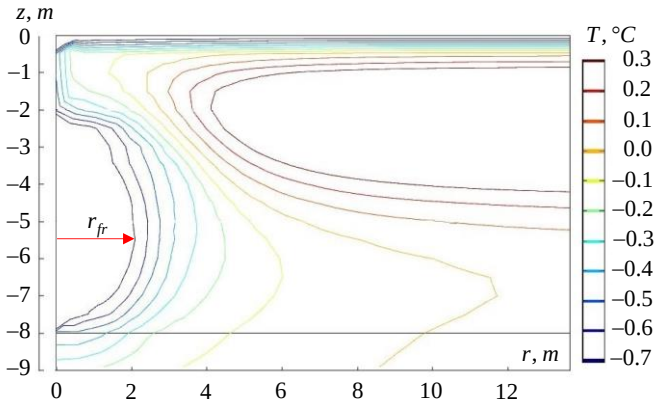

Fig. 5. The expected temperature distribution in the soil around the thermosyphon.

Fig.6 Ttemperature dynamics at the points $r=r_{fr}$ for proposed model & the model given in [12].

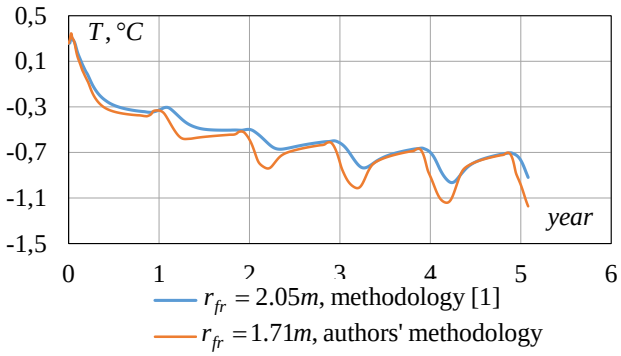

Figure 6. Temperature dynamic, distance $r=r_{fr}$ and z=-5m.

Mathematical investigation predicts that after 5 years, temperature of the soil in the proposed model, is 0.59 ºC at a distance r_{fr}=1.57 m from the central axis. At the same time, the calculation according to the model in [12] give the distancer_{fr} = 2.03 m. Thus, the calculation according to the authors' model of thermosyphon leads to reduction in the radius of freezing by 18%..

4. CONCLUSION

The investigator have developed the formula for analyzing the average film thickness of liquid refrigerant used on the inner surface & in all parts of the thermosyphon: condenser, overground pipe, underground heat insulated pipe, evaporator (23) – (26). The mathematical investigation predicts the thermal resistance of refrigerant film is second orders less as compare the thermal resistance of the condenser. Thus the experimental analysis for the temperature regime of soil is possible without considering the refrigerant film thickness. The expressions for analyzing absorbed ,direct, diffuse & reflected solar radiation by the condenser & over ground pipe is obtained (38). Useful data for a formula coincide with meteorological parametric range: direct normal irradiance, direct horizontal irradiance, diffuse horizontal irradiance, albedo of ground surface. Comparison of present model with the model given in [12] is done. The considerable difference between the models is found in the method of calculation of absorbed solar radiation in condenser and over ground pipe of a thermosyphon. The outcome analysis of two models of system two-phase thermosyphon – soil – atmosphere gives that the proposed model minimizing the freezing radius & the maximal gap between thermosyphons by 17%.

Nomenclatures

A_{surf}	albedo of ground surface, u.f.
b_{air}	back radiation factor of atmosphere, u.f.
c_{fr}	isobaric heat capacity of frozen soil, $Jkg^{-1}K^{-1}$
c_{soil}	isobaric heat capacity of soil, $Jkg^{-1}K^{-1}$
c_{th}	isobaric heat capacity of thawed soil, $Jkg^{-1}K^{-1}$
ed	absorbed diffuse solar radiation by condenser, W
$eref$	absorbed reflected solar radiation by condenser, W
er	absorbed solar radiation by condenser butt end, W
$esun$	Absorbed diffuse solar radiation by thermosyphon, W
fa	surface area of solar radiation diffusion in the atmosphere, m^{-2}
$fcon$	condenser area, m^{-2}
G	acceleration of gravity, m s^{-2}
G_{sun}	diffuse horizontal irradiance, Wm^{-2}
ha	vertical distance from the surface of the condenserto the surface of solar radiationdiffusion, m
J	flow of liquid refrigerant, kgs^{-1}
K_{con}	overall heat transfer coefficient of condenser, $Wm^{-1}K^{-1}$
K_{evp}	overall heat transfer coefficient ofevaporator, $Wm^{-1}K^{-1}$
K_{og}	overall heat transfer coefficient ofovergroundpipe, $Wm^{-1}K^{-1}$
K_{ug}	overall heat transfer coefficient ofundergroundpipe, $Wm^{-1}K^{-1}$
L_{rf}	heat of refrigerant vaporization, J kg^{-1}
L_w	heat of fusion, Jkg^{-1}
l_{con}	length ofcondenser, Wm^{-1}
l_{evp}	length ofevaporator, Wm^{-1}
l_{og}	length ofovergroundpipe, Wm^{-1}
l_{ug}	length ofundergroundpipe, Wm^{-1}
n_a	inner ground-normal vector
n_{con}	condenser surface normal vector
n_{surf}	outward ground-normal vector
Pr	Prundtl number of air, d.l.
Q_{inw}	inward heat flux on the surface of the ground, Wm^{-2}
Q_{sun}	global horizontal irradiance, Wm^{-2}
q_{con}	linearheatsourcein condenser, Wm^{-1}
q_{evp}	linearheatsourceinevaporator, Wm^{-1}
q_{og}	linearheatsourceinovergroundpipe, Wm^{-1}
q_t	linearheatsourceinthermosyphon, Wm^{-1}

q_{ug}	linearheatsourceinundergroundpipe, Wm^{-1}
R	distance from the surface of the condenserto the surface of solar radiationdiffusion, m
R_c	condenser radius, m
R_{ev}^{on}	evaporator radius, m
R_r^p	fin radius, m
R	projection of R on the surface of the ground, m
r_{fr}	radius of freezing, m
s	the distance between fins, m
S_N	surface of unfinned area of condenser, m^2
s_{su}	direct horizontal irradiance, Wm^{-2}
S'^{n}_{s}	direct normal irradiance, $W\ m^{-2}$
S_v^{un}	direct vertical irradiance, Wm^{-2}
T	time, s
T	temperature of soil, K
T_{ai}	temperature of air, K
T_{bf}^{r}	soil freezing point, K
T_g	temperatureofrefrigerantgaseous phase, K
T_{in}	soil freezing interval, K
V_a^t	wind speed, ms^{-1}
z_0	ground level, m
z_{ev}	top ofevaporator, m
z_{lo}^{p}	bottom ofthermosyphon, m
z_{up}^{w}	topofthermosyphon, m

reek Symbols

α_N	convective heat transfercoefficient for overground pipe, $W{\cdot}m^{-2}{\cdot}K^{-1}$
α_r	convective heat transfercoefficient for condenser fin, $W{\cdot}m^{-2}{\cdot}K^{-1}$
α_R	convective heat transfercoefficientfor side surface of condenser fin, $W{\cdot}m^{-2}{\cdot}K^{-1}$
α_{su}	convective heat transfercoefficient on the surface of
$_{rf}$	the ground, $W{\cdot}m^{-2}{\cdot}K^{-1}$
ψ_c	condenser wall thickness, m
Ψ_{ev}^{on}	evaporator wall thickness, m
ψ_r^p	refrigerant film thickness, m
Ψ_{r0}	initial refrigerant film thickness, m
Ψ_{ra}	average refrigerant film thickness, m
δ_{rc}	refrigerant film thickness in lowest point of condenser, m
Ψ_{re}	average refrigerant film thickness in evaporator, m
Ψ_{rc}^{a}	average refrigerant film thickness in condenser, m

Ψ_{ro}^{a}	average refrigerant film thickness in overground pipe, m
Ψ_{ru}^{a}	average refrigerant film thickness in underground pipe, m
Ψ_{sn}^{a}	snow thickness, m
γ_{con}^{ow}	emissivity of condenser surface, u.f.
γ_{og}	emissivity of overground pipe surface, u.f.
γ_{sur}	emissivity of ground surface, u.f.
Θ^{f}	angle in a cylindrical coordinate system, rad
η_a	thermal conductivity of air, W $m^{-1}K^{-1}$
η_{co}	thermal conductivity of condenser material, W $m^{-1}K^{-1}$
η_{evp}^{n}	thermal conductivity of evaporator material, W $m^{-1}K^{-1}$
η_{fr}	thermal conductivity of frozen soil, W $m^{-1}K^{-1}$
η_{hi}	thermal conductivity of heat insulation, W $m^{-1}K^{-1}$
η_R	thermal conductivity of material of finning, W $m^{-1}K^{-1}$
η_{rf}	thermal conductivity of refrigerant, W $m^{-1}K^{-1}$
η_{th}	thermal conductivity of thawed soil, W $m^{-1}K^{-1}$
ν_a	air viscosity, m^2s^{-1}
ν_{rf}	liquid refrigerant viscosity, m^2s^{-1}
ρ_{rf}	density of liquidrefrigerant, kgm^{-3}
ρ_{so}^{il}	density of soil, kg m^{-3}
ρ_{sk}	density of dry soil, kg m^{-3}
$\rho_{w,}^{tot}$	content of water in the soil, kg m^{-3}
$\rho_{w,}^{max}$	maximal content of water in the soil, kg m^{-3}
$\rho_{w,}^{nf}$	content of non-freezingwater in the soil, kg m^{-3}
ρ_{sn}^{ow}	density of the snow, kg m^{-3}
σ_0	Stefan Boltzmann's constant, W m^{-2} K^{-4}
φ_a	angle between R and n_a
φ_{co}^{n}	angle between R and n_{con}
$\nu\cdot$	divergence operator
V	gradient operator

REFERENCES

[1]. Lisin, Y.V.; Sapsaj, A.N.; Pavlov, V.V.; Zotov, M.Yu.; and Kaurkin, V.D. (2014). Selection of optimal solutions for laying an oil pipeline to ensure reliable operation of the Zapolyarye - NPS Pur-Pe based on thermal calculations.*Transportation and storage of petroleum products and hydrocarbons*, 1, 5-16.

[2]. Ershov, E.D. (1995). *Physical and chemical bases of permafrost studies*(1th ed.).Moscow: Lomonosov Moscowstate university.

[3]. Kalyuzhnyy, I.L.; and Lavrov, S.A. (2012). *Hydrophysical processes in the catch basin: Experimental studies and modeling*(1th ed.). St. Peterburg: Nestor-Istoriya.

[4]. Kutvitskaya, N.B.;and Minkin, M.A. (2014). Design of beds and foundations of infrastructure for oil-gas condensate fields under complex frozen-soil condition.*Soil Mechanics and Foundational Engineering*, 1, 21-25.

[5]. Markov, E.V.;Pulnikov, S.A.; and Sysoev, Yu.S. (2018). Evaluation of the effectiveness of ring thermal insulation for protecting a pipeline from the heaving soil.*Journal of Engineering Science and Technology*, 13(10), 3344-3358.

[6]. Fantozzi, F.; Filipeschi, S.; Mameli, M.; Nesi,S.;Cillari, G.; Mantelli,M.B.H.; andMilanez, F.H. (2017). An Innovative Enhanced Wall to Reduce the Energy Demand in Buildings.*Journal of Physics: Conference Series*, 796, 1-10.

[7]. Jafari, D.; Franco, A.; Filippeschi, S.; and Di Marco, P. (2016). Two-phase closed thermosyphons: A review of studies and solar applications.*Renewable and Sustainable Energy Reviews*, 53, 575-593.

[8]. Jadhav A.S.; and Patil S.A. (2016).Two phase thermosyphon - a review of studies.*International Journal of Engineering Sciences &Research Technology*, 5(1), 193-205.

[9]. Haan, V.O.; and Knudsen, K.D. (2019). Application of a two-phase thermosyphon loop calculation method to a cold neutron source.*Cryogenics*, 97, 55-62.

[10]. Haan, V.O.; René, G.; and Rowe J.M. (2017). Thermodynamic calculations of atwo-phase thermosyphon loop for cold neutron sources.*Cryogenics*, 85, 30–43.

[11]. Özbaş, E. (2019). Experimental study of thermal performance and pressure differences of different working fluids in two-phase closed thermosyphons usıng solar energy.*Journal of Polytechnic*, 22 (1), 121-128.

[12]. Gorelik, Y.B.;and Seleznev, A.A. (2016). About efficiency of the condenser finning of the short vertical thermostabilizer for building on permafrost.*Earth Cryosphere*, 10(2), 78-89.

[13]. Ali, K.K.; and Hassan, H.A. (2018). A Numerical - Experimental Study of Turbulent Heat Transfer Flow a Cross Square Cylinder In A Channel.*International Journal of Mechanical Engineering and Technology*, 9(8), 447–461.

[14]. Menni, Y.; Azzi, A.; and Zidani, C. (2017). Use of waisted triangular-shaped baffles to enhance heat transfer in a constant temperature-surfaced rectangular channel. *Journal of Engineering Science and Technology*, 12(12), 3251-3273.

[15]. Pathak, K.K.; Giri, A.;and Lingfa, P. (2017). Evaluation of heat transfer coefficient of a shrouded vertical array of heat sinks (fins): A computational approach.*International Journal of Mechanical Engineering and Technology*, 8(4), 319- 326.

[16]. Sidibé, M.; Soro, D.; Fassinou, W.F.;and Touré, S. (2017). Reconstitution of solar radiation on a site of the littoral in Cô te D'ivoire.*International Journal of Engineering Research and Technology*, 10(1), 19-34.

[17]. Markov, E.V.; Pulnikov, S.A.; and Sysoev, Y.S. (2018).Methodology for calculating the safe stop time of underground pipeline with high pour point oil.*International Journal of Civil Engineering and Technology*, 9(8), 1699-1705.

[18]. Markov, E.V.; Pulnikov, S.A.;and Sysoev, Y.S. (2018). Study of frost mound temperature condition.*International Journal of Civil Engineering and Technology*, 9(9), 10-15.

[19]. Markov, E.V.; Pulnikov, S.A.;and Sysoev, Y.S. (2018). Methodology for calibration of soil heat transfer model In accordance with results of measurements.*International Journal of Civil Engineering and Technology*, 9(9), 1721-1727.

[20]. Bhaskar, B.S.;and Choudhary, S.K. (2017). Experimental investigation of heat transfer through porous material heat exchanger.*International Journal of Engineering Research and Technology*, 10(1), 51-60.

[21].